

# Accelerated ReaxFF Simulations for Describing the Reactive Cross-Linking of Polymers

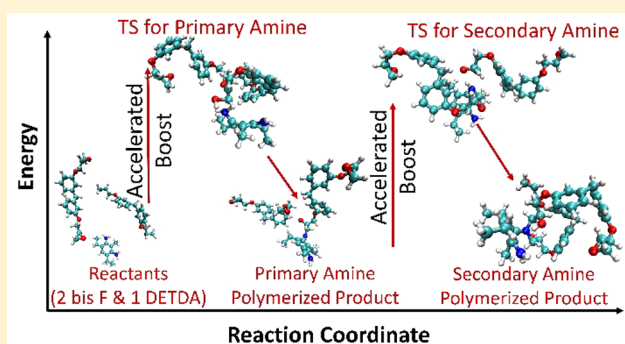
Aniruddh Vashisth,<sup>†</sup> Chowdhury Ashraf,<sup>#</sup> Weiwei Zhang,<sup>#</sup> Charles E. Bakis,<sup>†</sup> and Adri C. T. van Duin<sup>\*,†,#</sup>

<sup>†</sup>Department of Engineering Science and Mechanics, The Pennsylvania State University, 212 Earth and Engineering Sciences Building, University Park, Pennsylvania 16802, United States

<sup>#</sup>Department of Mechanical Engineering, The Pennsylvania State University, 136 Research East Building, Bigler Road, University Park, Pennsylvania 16802, United States

## Supporting Information

**ABSTRACT:** Various methods have been developed to perform atomistic-scale simulations for the cross-linking of polymers. Most of these methods involve connecting the reactive sites of the monomers, but these typically do not capture the entire reaction process from the reactants to final products through transition states. Experimental time scales for cross-linking reactions in polymers range from minutes to hours, which are time scales that are inaccessible to atomistic-scale simulations. Because simulating reactions on realistic time scales is computationally expensive, in this investigation, an accelerated simulation method was developed within the ReaxFF reactive force field framework. In this method, the reactants are tracked until they reach a nonreactive configuration that provides a good starting point for a reactive event. Subsequently, the reactants are provided with a sufficient amount of energy—equivalent or slightly larger than their lowest-energy reaction barrier—to overcome the barrier for the cross-linking process and form desired products. This allows simulation of cross-linking at realistic, low temperatures, which helps to mimic chemical reactions and avoids unwanted high-temperature side reactions and still allows us to reject high-barrier events. It should be noted that not all accelerated events are successful as high local strain can lead to reaction rejections. The validity of the ReaxFF force field was tested for three different types of transition state, possibly for polymerization of epoxides, and good agreement with quantum mechanical methods was observed. The accelerated method was further implemented to study the cross-linking of diglycidyl ether of bisphenol F (bis F) and diethyltoluenediamine (DETDA), and a reasonably high percentage (82%) of cross-linking was obtained. The simulated cross-linked polymer was then tested for density, glass transition temperature, and modulus and found to be in good agreement with experiments. Results indicate that this newly developed accelerated simulation method in ReaxFF can be a useful tool to perform atomistic-scale simulations on polymerization processes that have a relatively high reaction barrier at a realistic, low temperature.



## 1. INTRODUCTION

The mechanical properties of epoxy depend significantly on the molecular structure formed during polymerization. The cross-linked structure of an epoxy depends on various factors such as the specific epoxide and curing agent constituents, processing conditions, thermal history,<sup>1</sup> stoichiometry of constituents,<sup>2</sup> and degree of polymerization. Experiments have shown that the mechanical and thermal properties can vary significantly depending on the degree of cross-linking of the polymer as well as the polymer chemistry.<sup>3–8</sup> Thorough experimental investigation of these physical properties is expensive as it requires labor time and materials. Therefore, simulating these properties using molecular dynamics (MD) simulations has recently been considered<sup>9–11</sup> as an attractive alternative to the experiments as useful atomistic-level insight can be obtained from these simulations.

Simulating cross-linking of epoxy is a challenging task as polymerization of the constituent molecules to a vitreous state (roughly 75–80% complete) naturally occurs over a period of time ranging from a few minutes to days. At such times scales, atomistic-scale simulation of polymerization while capturing the correct chemical reactions is nearly impossible with current state-of-art computational methods. To overcome the computational time barrier, several methods have been proposed to achieve cross-linking at low computational expense. For example, coarse grain molecular simulations do not simulate all of the atomistic details and instead represent groups of atoms by beads or mesoparticles.<sup>12–15</sup> Another

Received: April 23, 2018

Revised: July 10, 2018

Published: July 11, 2018

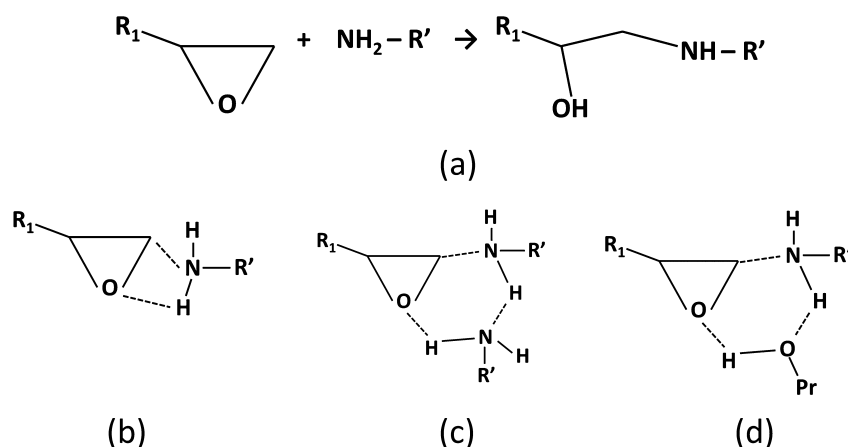


**Figure 1.** (a) Polymerization reaction of the epoxide and amine curing agent; transition state for the (b) noncatalyzed reaction, (c) self-promoted reaction, and (d) water-catalyzed reaction of epoxide and amine.

approach models polymerization at the atomic simulation level by monitoring distances between the reactive sites in the participating molecules.<sup>16–20</sup> Lin and Khare<sup>9</sup> extended this approach by developing a single-step polymerization method that minimizes the sum of the distances between the atoms forming the potential bonds. Yarovsky and Evans<sup>11</sup> and Bandyopadhyay et al.<sup>10</sup> proposed a similar cross-linking method where activated reactive sites were generated by breaking  $H_2C-O$  bonds and  $N-H$  bonds in epoxides and amine curing agents, respectively. The resulting  $CH_2$  ends were cross-linked with activated  $N$  atoms when the root-mean-square (RMS) distance between them was within a specified cutoff distance. Using the same approach, Odegard et al.<sup>21</sup> used nonreactive force field and cutoff methodology to cross-link polymers and equilibrated the system with reactive force field. Li and Strachan<sup>22</sup> developed a scheme that used the electronegativity equalization method (EEM)<sup>23</sup> to predict partial atomic charge progression during polymerization of epoxide and the curing agent. Kinetic Monte Carlo (kMC)<sup>24</sup> is a potential method to simulate reactions with slower reaction kinetics and has shown potential to simulate polymerization.<sup>25–27</sup> However, kMC is based on transition state rate constants that can locally vary in a system due to steric hindrance or a catalyst present in the system. kMC will treat all of the geometries similarly without considering the local strain buildup due to steric hindrances, which might change the reaction barrier significantly for a specific orientation. Additionally, to simulate the reaction between primary and secondary amines separately, as these reactions would have slightly different transition state rate constants, kMC will require separate inputs.

Essentially all thermoset simulations to date have been carried out with nonreactive interatomic potentials that do not enable bond breaking and formation. Additionally, those polymerization methods only consider the distance between the atoms of interests, i.e., whenever the distance falls within a certain limit, a bond is created without consideration of the effects of geometry and steric hindrance. Thus, the correct chemistry of polymerization reaction has never been studied using MD simulations. Because the entire polymerization process significantly affects the mechanical properties of the polymer, a comprehensive method is required to tackle the limitations of the earlier approaches<sup>9–11,21</sup> that includes the approach path of the reactive sites and influence of steric

hindrance during the reaction. Also, to avoid unwanted side reactions and to mimic experimental procedures, this method should be able to simulate the reactions at experimentally feasible temperatures. To atomistically simulate chemical reactions, development of accurate reactive force fields such as Reactive Empirical Bond Order (REBO) and ReaxFF<sup>28–30</sup> is required, which can enable the simulations to provide a deeper understanding of the reaction and postprocessing.

It is known that polymerization reaction of epoxy usually occurs when a nucleophilic amine nitrogen attacks usually on a terminal carbon of the epoxide molecule. The mechanism has been proposed to be  $S_N2$ -type II, and thus, the reaction rate obeys second-order kinetics.<sup>31</sup> These reactions may involve both primary and secondary amines as well as hydrogen-bonding catalysts and promoters, which exhibit a considerable effect on the activation barrier of the curing reaction. Primary polymerization of epoxide with an amine is shown in Figure 1a. Different types of polymerization reactions between epoxide and amine curing agent molecules can happen, including a noncatalyzed reaction, self-promoted reaction, and water-catalyzed reaction. The transition states for these reactions, as shown in Figure 1b–d, differ from each other, although the end product is the same.

For these three types of reactions, Ehlers et al.<sup>31</sup> calculated both the classical barrier energy and the activation energy ( $E_a$ ). The classical barrier energy is the difference in the total energies at the transition states and the corresponding reactants, whereas the activation energy is obtained by fitting the calculated rate constants to the Arrhenius expression,  $A \exp^{-E_a/RT}$ , where  $A$  is the pre-exponential factor that is a constant for each chemical reaction and  $R$  is the universal gas constant. The quantum mechanics (QM) calculations were carried out at the Density Functional Theory B3LYP level<sup>32</sup> with the 6-31G(d,p) basis set. The classical energy barrier for the noncatalyzed reaction (43.4 kcal/mol)<sup>31</sup> was found to be higher compared to the two catalyzed reactions as the six-membered ring transition states for the latter two reactions (33.4–35.7 kcal/mol)<sup>31</sup> are more stable than the four-membered ring for the noncatalyzed reaction. Similar reaction kinetics can be expected when translating to a larger system that contains epoxide resins and amine-based curing agents with a carbon-based backbone. For the reaction shown in Figure 1a, the groups  $R_1$  and  $R'$  are molecules with a carbon backbone.

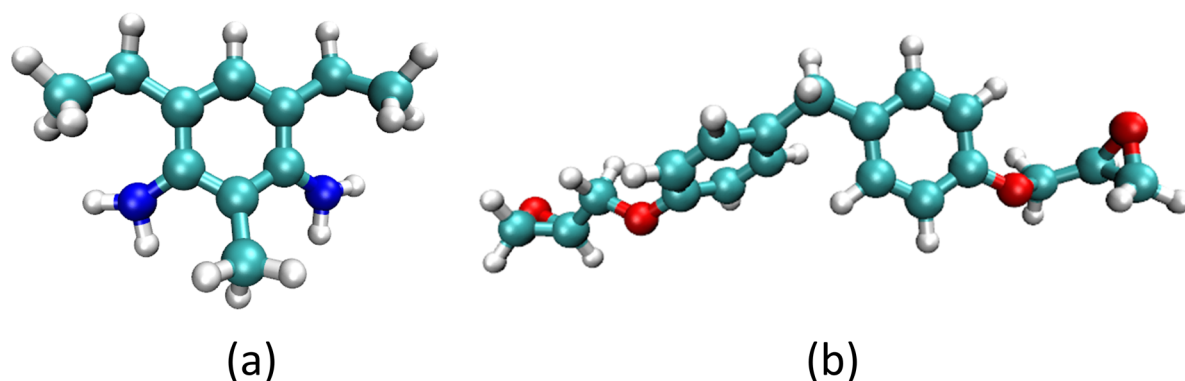


**Figure 2.** Molecules examined for polymerization of larger systems, (a) DETDA and (b) bis F. Cyan, red, blue, and white spheres represent carbon, oxygen, nitrogen, and hydrogen atoms, respectively.

In this investigation, EPON 862 (Hexion, Columbus, OH) which is a diglycidyl ether of bisphenol F (bis F) epoxide, was cured with EPIKURE W/Curing agent W (Miller-Stephenson, Danbury, CT) which is diethyltoluenediamine (DETDA). The molecular configurations of bis F and DETDA are shown in Figure 2.

Cross-linking of epoxide polymers with amine curing agents can be accelerated by elevated temperatures during experiments. The challenging part of simulating these reactions is to get high cross-linking density, as observed in experiments. Whereas a low cross-linked polymer would limit the simulation accuracy, a highly cross-linked “perfect” network will almost inevitably yield an overestimate of modulus and strength. Shenogina et al.<sup>33</sup> studied epoxy networks and confirmed this observation using MD simulations. A highly cross-linked perfect network would be impossible to produce experimentally as the steric hindrance due to long polymer chains would restrict the reactions between the reactive sites in the epoxide and the amine remaining after vitrification.

Because a high degree of polymerization (up to 75–90% cross-linking) could take a significant amount of time (experimental time scales are typically several minutes), it cannot be simulated using standard ReaxFF at a reasonable simulation time because standard ReaxFF time scales are typically in the nanosecond range. In this investigation, a novel method is developed within the ReaxFF reactive force field framework to accelerate the cross-linking reaction by providing a sufficient amount of energy, based on the distances and orientations of the reactants to help the reactants overcome the reaction barrier. A similar method was previously used to successfully accelerate the kinetics of slower reactions.<sup>34</sup> This newly developed ReaxFF accelerated method first calculates the distances between atoms that are relevant to the cross-linking reaction to determine the orientation of the reactant molecules. If a suitable initial configuration is recognized, it then provides additional energy to the system by stretching or compressing bonds at a predefined rate such that this additional energy can help achieve the energy to cross the energy barrier of the polymerization.

## 2. METHODS

**2.1. Experimental Methods.** Bis F epoxide and DETDA were mixed in a 100:26.4 stoichiometric ratio, and dogbone specimens were cast in an aluminum mold by curing the mixture for 1 h at 121 °C followed by postcuring for 3.5 h at 177 °C. The tensile modulus ( $E$ ), density ( $\rho$ ), and glass

transition temperature ( $T_g$ ) of the epoxy were measured. The tensile modulus was measured using four dogbone specimens with two clip gages on opposite sides of the specimen measuring the average strain in the loading direction and one clip gage measuring strain in the transverse direction. A straight line was fit to the stress and strain data by the least-square method over a longitudinal strain range of 0–2500  $\mu\epsilon$  to compute the modulus. Shavings of matrix specimens were used to measure  $T_g$  using modulated differential scanning calorimetry (MDSC) with a TA Instruments DSC Q2000 (New Castle, DE). Each specimen was scanned three times, and the inflection point of each ramp was used for calculating the  $T_g$ . The average of three ramps is reported as the  $T_g$ . The densities were measured in accordance with ASTM D792<sup>35</sup> with five specimens. Vashisth and Bakis<sup>8</sup> detail the experimental procedures for all tests carried out for matrix characterization.

**2.2. Computational Details.** ReaxFF is a reactive force field MD simulation technique that uses the bond order concept to consider the instantaneous interaction between atoms.<sup>28,36</sup> It provides a smooth transition between the nonbonded states and single, double, or triple bonded states. This strategy allows one to investigate the chemical reactions where bond formation and bond dissociation are involved during simulation. In general, the total interaction energy in ReaxFF is described by several contributions and can be summed up as follows

$$E_{\text{system}} = E_{\text{bond}} + E_{\text{over}} + E_{\text{under}} + E_{\text{val}} + E_{\text{tors}} + E_{\text{vdW}} + E_{\text{Coulomb}} + E_{\text{lp}} + E_{\text{H-bond}} + E_{\text{rest}} \quad (1)$$

The total energy of the system ( $E_{\text{system}}$ ) consists of bonded or covalent interactions (which are bond-order-dependent) and nonbonded interactions. Bond-order-dependent terms include the bond energy ( $E_{\text{bond}}$ ), overcoordination ( $E_{\text{over}}$ ), undercoordination ( $E_{\text{under}}$ ), and hydrogen bond ( $E_{\text{H-bond}}$ ) interactions. Energy penalty terms include torsion angle energy ( $E_{\text{tor}}$ ), valence angle energy ( $E_{\text{val}}$ ), and lone pair energy ( $E_{\text{lp}}$ ). Nonbonded interactions include van der Waals ( $E_{\text{vdW}}$ ) and Coulomb energy ( $E_{\text{Coulomb}}$ ). Bond order is directly calculated between all pairs of atoms from the interatomic distance and is updated at every MD or energy minimization step. Also, nonbonded interactions such as van der Waals and Coulomb terms are taken into account for all atom pairs. Atomic charges are derived from an EEM.<sup>23</sup> Force field parameters describing energy terms are typically optimized by QM calculations and

experimental values. ReaxFF has been successful in simulating processes pertaining to combustion reactions,<sup>36,37</sup> metal–water reactions,<sup>38</sup> nanomechanics of protein bonds,<sup>39</sup> thermal decomposition of polymers,<sup>40</sup> electrolyte reactions,<sup>41</sup> and mechanical responses<sup>42</sup> of batteries, 2-D materials,<sup>43</sup> metal oxides,<sup>44</sup> etc.

The restrain energy ( $E_{\text{rest}}$ ) denotes the external energy that is provided to atoms during the accelerated simulation. The additional energy provided to the system is the sum of restrain energies provided to various pairs of atoms. The restrain energy ( $E_{\text{rest}}$ ) is given by eq 2

$$E_{\text{rest}} = F_1 \{1 - e^{-F_2(R_{ij}-R_{12})^2}\} \quad (2)$$

where  $E_{\text{rest}}$  is the restrain energy between two atoms in kcal/mol,  $F_1$  and  $F_2$  are force parameters for restrain energy with units of kcal/mol and  $\text{\AA}^{-2}$ , respectively,  $R_{12}$  is the desired distance (in  $\text{\AA}$ ) between two atoms according to restrain, and  $R_{ij}$  is the actual distance (in  $\text{\AA}$ ) between two atoms under consideration. It is essential to choose the correct values of the restrain energy parameters that provide optimum energy for cross-linking. The procedure to select the values of the force constants will be discussed in the following sections.

To describe the reaction between epoxide and amine, reoptimization of the force field was carried out based on the parameters of CHNO-2017\_weak,<sup>45</sup> which was developed to improve the description of functionalized hydrocarbon/water weak interaction in the condensed phase. It has been demonstrated that the CHNO-2017\_weak force field can reproduce the properties of the functionalized hydrocarbon system and the hydrocarbon–water mixtures. In the force field reparameterization procedure, the parameters related to the hydrocarbons and the water molecules in the CHON-2017\_weak force field were kept the same, but the parameters for C–O, C–N, and N–H bond terms, angle terms of oxygen and nitrogen atoms, and the hydrogen bonding parameters of nitrogen were optimized to improve their reproduction of epoxide/amine coupling reactions. The reoptimized force field used in this investigation can be found in the [Supporting Information](#).

### 2.3. Simulation Procedure. Polymerization Strategy.

The “bond-boost method” that was developed by Miron and Fichthorn<sup>34</sup> was studied and partially applied to ReaxFF for accelerated simulations. The accelerated approach used in this investigation first identifies the atoms in particular molecules that may participate in a reaction. Equilibrium configurations of these tagged atoms are determined, and an extra potential in terms of additional energy is added to these atoms during the standard MD simulations. This additional energy is used to stretch or compress the bonds associated with the identified atoms. The stretching of bonds is associated with the atoms that break bonds during the reaction, whereas the compressing is associated with the atoms that form new bonds. When the system jumps to a new minimum, the extra potential automatically goes to zero and remains there.

Application of the accelerated approach to ReaxFF is done by applying extra potentials to multiple pairs of atoms using the restrain energy ( $E_{\text{rest}}$ ), which is calculated in terms of the atomic distances ( $R_{12}$ ) and two force parameters ( $F_1$  and  $F_2$ ). Whenever the spatial configurations of marked atoms are satisfied, an additional energy will be generated that is dependent on the chosen force parameters. This is done in a manner that the restrain energy is comparable to the energy

required by the system to overcome the reaction barrier. Therefore, a systematic analysis was carried out by running various NVT simulations with a wide range of force parameters ( $F_1$ ,  $F_2$ , and  $R_{12}$ ), and the approximate barrier energy was calculated by subtracting the energy of the transition state from the initial energy of the system. This was tested for noncatalyzed, water-catalyzed, and self-promoted reactions. Next, transition state structures with a minimum barrier energy for different types of polymerization reactions were examined. Because the transition state is a saddle point, the system should only have one negative frequency. ReaxFF initial approximations of the barrier energy, based on simple bond stretching and compression using restraints, are fairly crude; thus, almost all of the cases ended up with multiple negative frequencies for the transition state structure. Using an in-house python code,<sup>37</sup> the structure was reduced to have only one negative frequency, therefore providing a better approximation for the reaction barrier in ReaxFF. The energy barriers generated using ReaxFF were compared to QM calculations available in the literature.<sup>31</sup> The force parameters that produced an energy barrier close to this ReaxFF calculation were selected for accelerated simulations of larger systems later in this investigation. For the sake of simplicity, this initial examination was carried out for representative systems containing epoxide and ammonia molecules with catalysts in some cases.

For polymerization using the accelerated approach in ReaxFF, atoms in the reactive sites that would take part in the reaction are initially identified. For example, the simplest case of an epoxide and ammonia is shown in [Figure 3](#). During

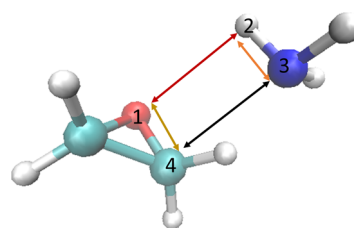


**Figure 3.** Constraints for an accelerated reaction between epoxide and ammonia (The color scheme is gray spheres, hydrogen; red spheres, oxygen; cyan spheres, carbon; and blue spheres, nitrogen).

an NVT simulation, the distances between O (atom #1) and H (atom #2), H (atom #2) and N (atom #3), N (atom #3) and C (atom #4), and finally C (atom #4) and O (atom #1) should fall within specified distances. If all three cutoff distances are satisfied, an extra potential is provided to the system by adding energy through the  $E_{\text{rest}}$  term. Subsequently, this extra potential is maintained for a certain number of MD time steps (10 000 steps of 0.25 fs in this investigation). It should be noted that not all accelerated cases lead to a successful reaction. Some cases revert to the initial configuration once the extra potential is removed (so reactions are not automatically successful), and the local structure affects the success of the polymerization step. The algorithm for all of the accelerated simulation examined is shown in [Figure 4](#).

It should be noted that for all of the accelerated polymerization reaction, only the carbon atom in the epoxide ring that is farther away from the chain was considered to bond with an attacking N atom. The rate of reaction for this specific carbon atom is twice as large compared to a carbon atom in the epoxide ring that is closer to the polymer backbone.<sup>31</sup> These



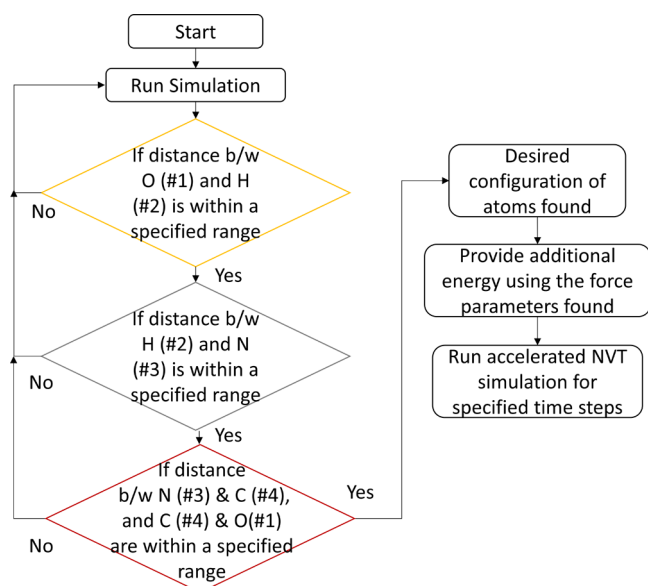


Figure 4. Flowchart for application of accelerated simulation.

differences arise from steric hindrances in the reaction of the reactive sites.

The polymerization methodology for a large system containing bis F and DETDA molecules is a multistep process. Initially, two bis F and one DETDA molecules are put in a system with an approximate density of  $0.4\text{--}0.6\text{ g/cm}^3$ . The system is simulated with NVT at 500 K using accelerated simulation potentials to drive the polymerization. Two polymers formed in the last step of this initial simulation are then placed in another system with a similar density of  $\sim 0.4\text{--}0.6\text{ g/cm}^3$  and accelerated, NVT simulations are carried out at 500 K. This procedure is carried out by doubling the number

of atoms at every step but keeping the stoichiometry the same throughout the process. The number of iterations to get cross-linking at every step varies depending on the size of the system. Smaller systems satisfy configurational requirements for accelerated simulations much faster as compared to systems with bulkier molecules. The final polymer was a continuous chain made up of 1872 atoms, i.e., 32 bis F and 16 DETDA molecules.

**Polymer Analysis.** The final polymer formed was analyzed to determine the density, glass transition temperature, and tensile modulus. To eliminate the problem of local concentrations in density, an annealing procedure was carried out to the initial structure. The procedure involved increasing the temperature of the structure from 300 to 600 K by an increment of 100 K (in 12.5 ps) and then cooling it down to 300 K and performing NPT between each temperature change at each interval for 12.5 ps. The density of the polymer was calculated from the last NPT cycle at 300 K. The whole procedure had a total of six NVT simulations and six NPT simulations.

The density of the annealed polymer was calculated by running NPT simulations over 10 different temperatures between 300 and 500 K at an interval of 20 K. Each NVT simulation had 50 000 time steps of 0.25 fs, and the NPT simulations had 200 000 time steps of 0.25 fs. The glass transition temperature was calculated by finding the intersection of two straight lines fitted by linear regression to the densities for the first five and last five temperatures.

Because it is difficult to simulate the strain rates at which the experimental tensile modulus was measured, higher strain rate testing was carried out in the MD simulations. Two strain rates were used to simulate the tensile mechanical testing of the polymer. The strain rates examined,  $2 \times 10^8$  and  $1 \times 10^8\text{ s}^{-1}$ , are similar to the rates examined by Odegard et al.<sup>21</sup> Because the elastic response of the polymer is a function of the strain

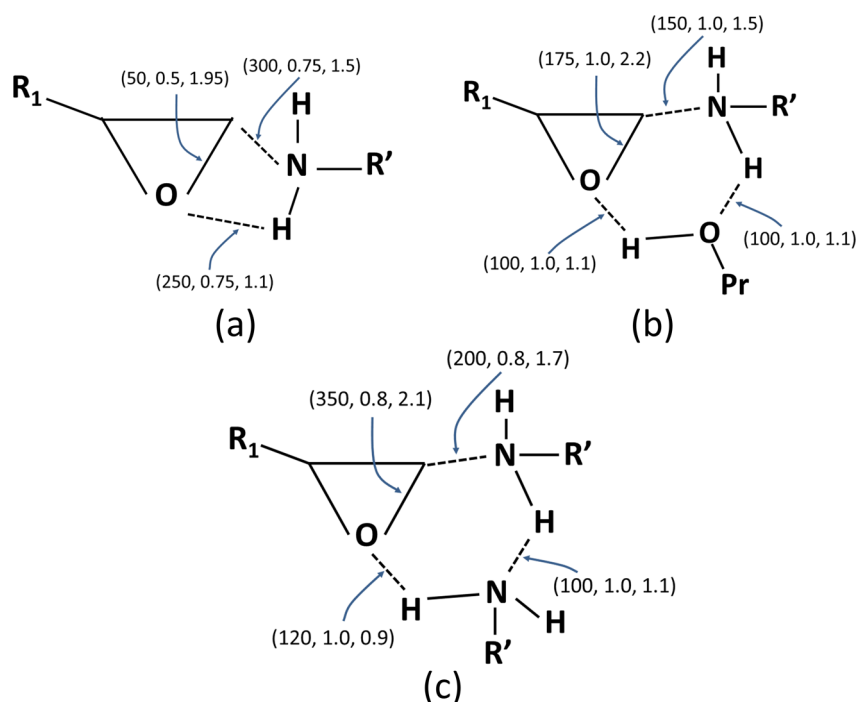


Figure 5. Force constants ( $F_1$  and  $F_2$ ) and target distances ( $R_{12}$ ) for three different types of possible reactions shown in parentheses as ( $F_1$ ,  $F_2$ ,  $R_{12}$ ) with units of kcal/mol,  $\text{\AA}^{-2}$ , and  $\text{\AA}$ , respectively.

rate, multiple strain rates were considered from experiments and simulations to fit a regression curve. These high strain rates were applied by changing the box size, with the constraint that the box shape always remains cuboidal. The four faces that were parallel to the strain direction were free to approach each other due to Poisson's effect. The Large-scale Atomic/Molecular Massively Parallel Simulator (LAMMPS)<sup>46</sup> was used to simulate tensile testing at 300 K with the "compute stress/atom command"<sup>47</sup> using ReaxFF in LAMMPS. Each system was tested in all three orthogonal directions, and the average of these three simulations is presented in the Results section.

### 3. RESULTS

#### 3.1. Force Parameters for Accelerated Simulations.

Transition states for three different types of reactions were examined and compared to QM data. Different sets of parameters were evaluated for noncatalyzed, water-catalyzed, and self-promoted reactions, respectively. Force parameters ( $F_1$  and  $F_2$ ) and target distances ( $R_{12}$ ) that gave the lowest barrier energy are shown in Figure 5 for the various bonds. Using these force parameters, an approximate barrier energy was calculated. These transition state structures have multiple negative frequencies, which are then used as an input for the Python code to come up with a nearby structure with only one significant negative frequency and thus a better approximation for the transition state structures. The Supporting Information provides the various force parameters that were evaluated for possible reaction. This information has been added under a separate section "Force Parameters". Another subroutine (tracking.in) that was developed for ReaxFF was added to the Supporting Information under the section "Tracking Subroutine: "Tracking.in". This subroutine enforces the proximity conditions and provides specific atoms with additional energy to cross over the energy barrier.

**3.2. Comparison to Quantum Mechanics (QM).** Ehlers et al.<sup>31</sup> presented the activation and the classical barrier energies of all of the different types of polymerizations considered in this investigation. The ReaxFF barriers were in good agreement with the QM numbers for the noncatalyzed polymerization, the water-assisted polymerization, and the self-assisted polymerization, as seen in Figures 6 and 7. Also, the distances shown in these two figures represent the atom distances at the transition state using ReaxFF. Good agreement

between QM and ReaxFF barriers was found for both the catalyzed and the noncatalyzed polymerization reactions.

**3.3. Bis F/DETDA Polymer.** Because the comparison between the ReaxFF and the QM energies for the epoxide and ammonia system shows good agreement and a polymer can be formed by providing an accurate amount of energy, it is established that accelerated simulation is a more thermodynamically accurate method as compared to previous investigations.<sup>9–11</sup> Now a larger system of bis F and DETDA can be studied using the accelerated ReaxFF simulation. For bis F/DETDA polymerization, the force parameters ( $R_{12}$ ,  $F_1$ , and  $F_2$ ) for O–C bonds were 1.95 Å, 50 kcal/mol, and  $0.5 \text{ Å}^{-2}$ , those for O–H were 1.1 Å, 250 kcal/mol, and  $0.75 \text{ Å}^{-2}$ , and those for C–N were 1.5 Å, 300 kcal/mol, and  $0.75 \text{ Å}^{-2}$ .

For polymerization, two bis F molecules and one DETDA molecule were simulated as mentioned earlier. The additional energy to drive the reaction versus time graph for this system is shown in Figure 8. The additional energy is the sum of all of the restrain energies that are applied on various pairs of atoms. The force parameters used in this system were the same as that of the noncatalyzed polymerization (Figure 5a). It can be observed that in various instances the conditions for the accelerated simulations are fulfilled but numerous non-successful attempts are applied that do not result in polymer formation. This result is due to the reaction reverting to the reactants rather than forming the desired product from the unstable transition state. The additional energy provided to the system goes to zero after a certain number of steps (10 000 steps of 0.25 fs in this study), and the system reverts back to simple NVT simulations until the spatial requirements for accelerated simulations are satisfied again. This is consistent with the "bond-boost" approach developed by Miron and Fichthorn.<sup>34</sup> It should be noted that a higher degree of cross-linking can be forced on the system by using stronger force parameters (i.e., inputting higher additional energy in the system), using larger cutoff distances between participating atoms, changing the temperature of the system, and running the system over an extensively long period of time. The motivation in this study was to get cross-linking with the least amount of additional energy provided to the system.

The final chained formed after four accelerated simulations, where the number of atoms was doubled in every simulation, as discussed in the Polymerization Strategy subsection. This method of cross-linking is not time-expensive as the simulations involving two bis F and one DETDA and four bis F and two DETDA molecules were relatively fast (5–6 CPU hours). The final polymer analyzed in this investigation had 32 bis F and 16 DETDA molecules that have 1872 atoms. The final polymer formed had an 82% cross-linked density. The cross-linked density is the percentage of the ratio of C–N bonds formed and possible C–N bonds that can be formed. NPT simulation at 300 K resulted in a  $0.83 \text{ g/cm}^3$  density. This density was low as the final structure had local variations of high and low densities. To eliminate this problem of local variations in density, an annealing procedure was carried out on the initial structure. The procedure involved increasing the temperature of the structure from 300 to 600 K by an increment of 100 K (in 12.5 ps.) and then cooling it down to 300 K and performing NPT between each temperature change at each interval for 12.5 ps. This can be seen in Figure 9, where the increase in temperature from 300 to 600 K occurred in three steps and in between these steps NPT simulations were

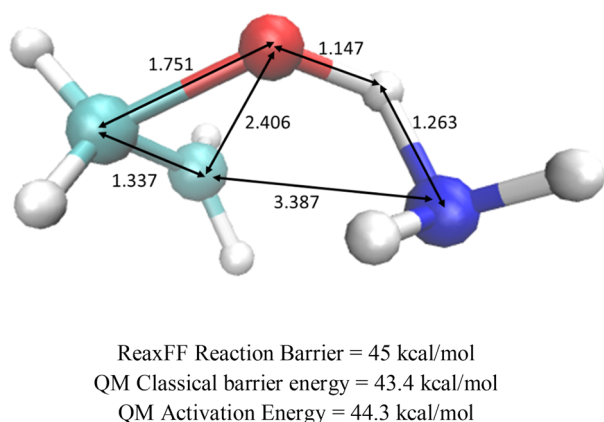


**Figure 6.** Transition state structures of noncatalyzed polymerization and comparison of ReaxFF and QM energies (distances in Å).

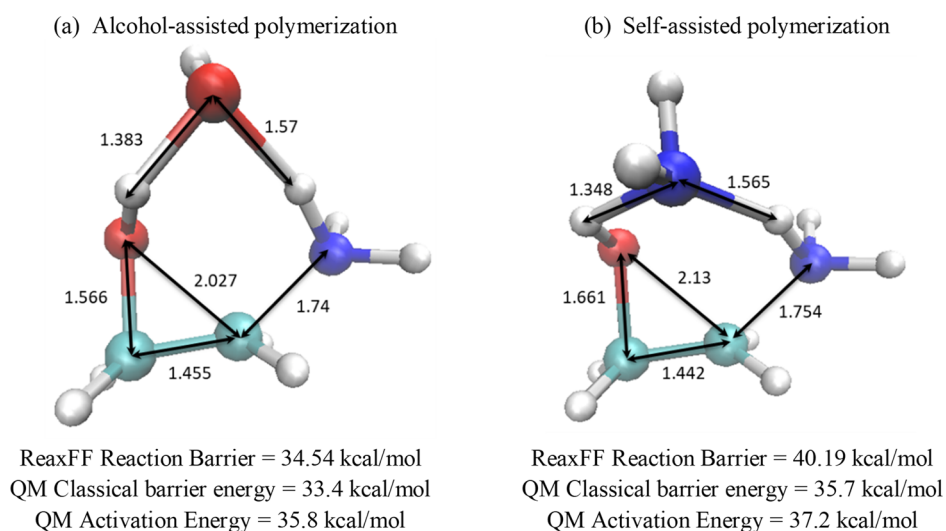


**Figure 7.** Transition state structures of (a) alcohol-assisted polymerization and (b) self-assisted polymerization and comparison of ReaxFF and QM energies (distances in Å).

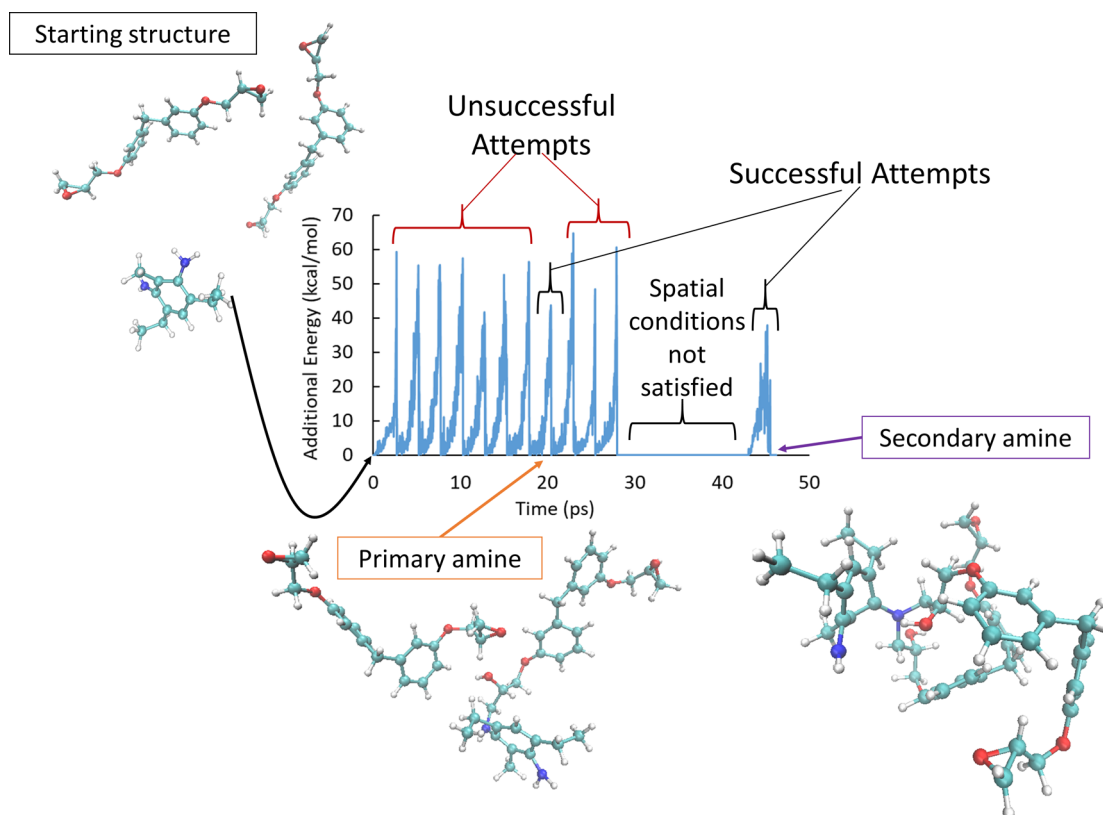


**Figure 8.** Additional energy provided to the bis F/DETDA system as a function of time. The graph shows successful and unsuccessful boost attempts.

carried out. This procedure has a total of six *NVT* simulations and six *NPT* simulations.

After the second annealing cycle, the final polymer density was  $1.167 \pm 0.010$  g/cm<sup>3</sup> for the 82% cross-link density. This simulated density is very close to the experimentally determined density of 1.185 g/cm<sup>3</sup>. Next, the tensile modulus of the cross-linked polymer was simulated using ReaxFF in LAMMPS. Two strain rates ( $2 \times 10^8$  and  $1 \times 10^8$  s<sup>-1</sup>) were used to simulate the tensile mechanical testing of the polymer along all three directions (*x*, *y*, and *z*). Figure 10b shows a

representative stress–strain curve for the cross-linked polymer. It should be noted that the fluctuations in the stress–strain graph are due to the significant vibrations that atoms experience at the atomistic scale.

Decent agreement between the extrapolated experimental modulus and the simulated modulus was found. Figure 10a shows the experimental data from Littell et al.<sup>48</sup> and the measured data in this investigation as well as simulated data from MD. The simulated moduli are  $5.0 \pm 0.6$  and  $6.1 \pm 1.9$  GPa for slow and fast strain rates, respectively. The modulus of

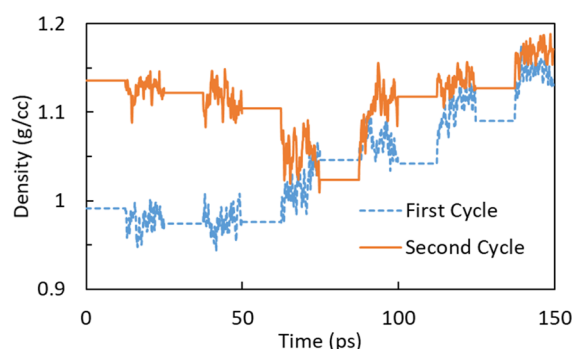


Figure 9. Density of the polymer during the annealing procedure.

the polymer was found to be different in the simulated tension tests in three orthogonal directions. This difference can be attributed to local heterogeneities as well as the spatial arrangement of the molecules within the tested box. Interestingly, the stress–strain graph of the bis F/DETDA polymer (Figure 10b) shows a characteristic yielding of the polymer at 0.03 strain or 3% strain, which is close to the experimental yield strain reported in the literature<sup>48</sup> for slower strain rates.

Next, the glass transition temperature of the simulated polymer is examined. It can be observed that densities decrease with increasing temperature. The temperature dependence of densities given in Figure 11 were calculated by averaging all of the calculations from the *NPT* simulations. The scatter bars represent the standard deviation in the density for a particular *NPT* at a particular temperature.

For the given graph in Figure 11, two linear regression lines were plotted for data points in the temperature ranges of 300–400 and 400–500 K. The intersection of these two lines provides the glass transition temperature ( $T_g$ ) for the simulated polymer. The measured glass transition temperature was found to be 423 K (150 °C), whereas the simulated  $T_g$  was found to be 409 K (136 °C). This is close to the range of  $T_g$  values simulated by Bandyopadhyay et al. (2011) of 416–430 K (143–157 °C) for a 76% cross-linked structure. The differences in the simulated  $T_g$  in this investigation and that from Bandyopadhyay et al.<sup>10</sup> can be explained by different force fields used for simulating the polymer and the different cross-linked densities of the simulated polymers.

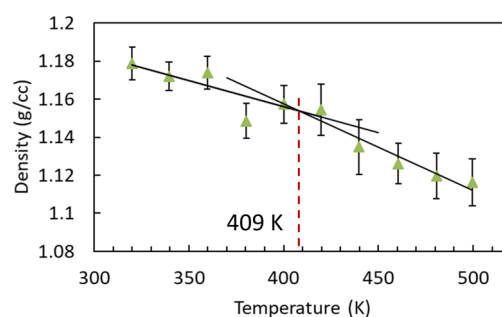


Figure 11. Density vs temperature graph for calculating the glass transition temperature.

#### 4. CONCLUSIONS

Polymerization of epoxide and amines requires additional energy to overcome the reaction barrier to form the transition state and further progress toward the products. The relatively high barriers for typically polymerization reactions make them inaccessible for regular reactive force field-based MD simulations. In this investigation, an accelerated method was developed within the framework of the ReaxFF reactive force field to simulate cross-linking of epoxide and amine molecules that allows the reactants to overcome the barrier. The energy barriers calculated using ReaxFF and QM were found to be in good agreement for all types of epoxide–amine polymerization reactions, namely, noncatalyzed, water-catalyzed, and self-catalyzed reactions. This accelerated approach was implemented by providing sufficient energy in the reactive sites of larger molecules, namely, bisphenol F and DETDA, to overcome the barriers for the polymerization reaction. This additional energy that enables bond breaking and formation was achieved by compressing or elongating the bonds between multiple pairs of atoms. It was observed that there were unsuccessful attempts for the reaction due to steric hindrances or inappropriate path of approach for the reactive molecules, whereas polymerization was achieved for the least resistant pathway for the reaction. To develop the polymer chain more efficiently, the accelerated reactions were carried out in a manner such that the number of molecules was doubled at each stage while the stoichiometry was kept constant. The polymer formed through this cross-linking method was 82% cross-linked, and that through virtual testing was shown to have a tensile modulus, glass transition temperature, and density close to those from experimental measurements.

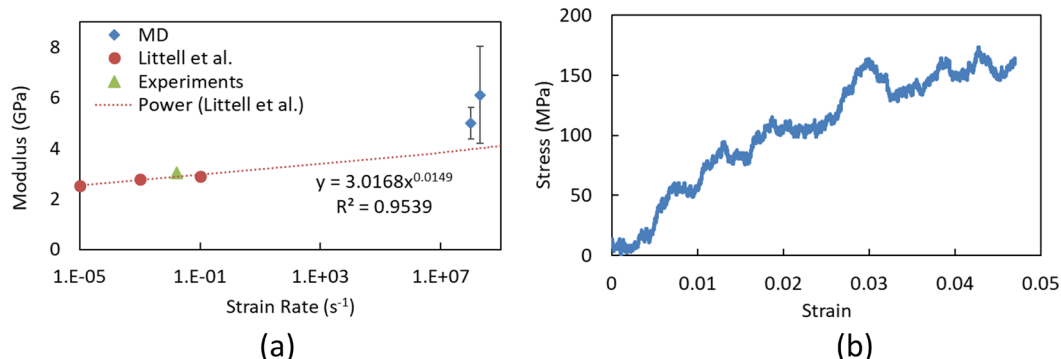


Figure 10. (a) Experimental and simulated modulus (simulation results as presented as avg.  $\pm$  std. dev) and (b) representative stress–strain curve for bis F/DETDA at a strain rate of  $1 \times 10^8 \text{ s}^{-1}$ .



This accelerated method provides an essential tool to simulate cross-linking that takes into account the barrier energy for slow reactions using reactive force fields. Using the accelerated simulations method, slower reactions such as oxidation of iron, fermentation of sugar into alcohol, chemical weathering of rocks, and even the photosynthesis process can be analyzed with the knowledge of barrier energies.

## ■ ASSOCIATED CONTENT

### ● Supporting Information

The Supporting Information is available free of charge on the ACS Publications website at DOI: [10.1021/acs.jpca.8b03826](https://doi.org/10.1021/acs.jpca.8b03826).

ReaxFF force field, tracking successful reaction, force parameters, and tracking subroutine (PDF)

## ■ AUTHOR INFORMATION

### Corresponding Author

\*E-mail: [acv13@engr.psu.edu](mailto:acv13@engr.psu.edu).

### ORCID

Aniruddh Vashisth: [0000-0002-4740-1296](https://orcid.org/0000-0002-4740-1296)

Weiwei Zhang: [0000-0002-5255-7340](https://orcid.org/0000-0002-5255-7340)

Adri C. T. van Duin: [0000-0002-3478-4945](https://orcid.org/0000-0002-3478-4945)

### Notes

The authors declare no competing financial interest.

## ■ ACKNOWLEDGMENTS

Cyberscience at Penn State is acknowledged for seed funding. This work was partially supported by a grant from the U.S. Army Research Laboratory through the Collaborative Research Alliance (CRA) for Multi-Scale Multidisciplinary Modeling of Electronic Materials (MSME). This research is partially funded by the Government under Agreement No. W911W6-11-2-0011. The U.S. Government is authorized to reproduce and distribute reprints notwithstanding any copyright notation thereon. The views and conclusions contained in this document are those of the authors and should not be interpreted as representing the official policies, either expressed or implied, of the U.S. Government.

## ■ REFERENCES

- (1) Meyer, F.; Sanz, G.; Eceiza, A.; Mondragon, I.; Mijović, J. The Effect of Stoichiometry and Thermal History during Cure on Structure and Properties of Epoxy Networks. *Polymer* **1995**, *36*, 1407–1414.
- (2) Levita, G.; De Petris, S.; Marchetti, A.; Lazzeri, A. Crosslink Density and Fracture Toughness of Epoxy Resins. *J. Mater. Sci.* **1991**, *26*, 2348–2352.
- (3) Nielsen, L. E. Cross-Linking—Effect on Physical Properties of Polymers. *J. Macromol. Sci., Polym. Rev.* **1969**, *3*, 69–103.
- (4) Ellis, B.; Found, M. S.; Bell, J. R. Influence of Cure Treatment on Extent of Reaction and Glassy Modulus for BADGE-DDM Epoxy Resin. *J. Appl. Polym. Sci.* **2001**, *82*, 1265–1276.
- (5) Enns, J. B.; Gillham, J. K. Effect of the Extent of Cure on the Modulus, Glass Transition, Water Absorption, and Density of an Amine-Cured Epoxy. *J. Appl. Polym. Sci.* **1983**, *28*, 2831–2846.
- (6) Detwiler, A. T.; Lesser, A. J. Aspects of Network Formation in Glassy Thermosets. *J. J. Appl. Polym. Sci.* **2010**, *117*, 1021–1034.
- (7) Morel, E.; Bellenger, V.; Bocquet, M.; Verdu, J. Structure-Properties Relationships for Densely Cross-Linked Epoxide-Amine Systems Based on Epoxide or Amine Mixtures. *J. Mater. Sci.* **1989**, *24*, 69–75.
- (8) Vashisth, A.; Bakis, C. E. Characterization of Nanosilica Filled Bis F Epoxide with Diamino Diphenyl Sulfone Curing Agents. In *31st*

*Technical Conference of the American Society for Composites*; Destech Publications: Williamsburg, VA, 2016; p 15.

(9) Lin, P.-H.; Khare, R. Molecular Simulation of Cross-Linked Epoxy and Epoxy-POSS Nanocomposite. *Macromolecules* **2009**, *42*, 4319–4327.

(10) Bandyopadhyay, A.; Valavala, P. K.; Clancy, T. C.; Wise, K. E.; Odegard, G. M. Molecular Modeling of Crosslinked Epoxy Polymers: The Effect of Crosslink Density on Thermomechanical Properties. *Polymer* **2011**, *52*, 2445–2452.

(11) Yarovsky, I.; Evans, E. Computer Simulation of Structure and Properties of Crosslinked Polymers: Application to Epoxy Resins. *Polymer* **2002**, *43*, 963–969.

(12) Stevens, M. J. Manipulating Connectivity to Control Fracture in Network Polymer Adhesives. *Macromolecules* **2001**, *34*, 1411–1415.

(13) Tsige, M.; Lorenz, C. D.; Stevens, M. J. Role of Network Connectivity on the Mechanical Properties of Highly Cross-Linked Polymers. *Macromolecules* **2004**, *37*, 8466–8472.

(14) Marrink, S. J.; Risselada, H. J.; Yefimov, S.; Tieleman, D. P.; de Vries, A. H. The MARTINI Force Field: Coarse Grained Model for Biomolecular Simulations. *J. Phys. Chem. B* **2007**, *111*, 7812–7824.

(15) Komarov, P. V.; Yu-Tsung, C.; Shih-Ming, C.; Khalatur, P. G.; Reineker, P. Highly Cross-Linked Epoxy Resins: An Atomistic Molecular Dynamics Simulation Combined with a Mapping/Reverse Mapping Procedure. *Macromolecules* **2007**, *40*, 8104–8113.

(16) Grest, G. S.; Kremer, K. Statistical Properties of Random Cross-Linked Rubbers. *Macromolecules* **1990**, *23*, 4994–5000.

(17) Doherty, D. C.; Holmes, B. N.; Leung, P.; Ross, R. B. Polymerization Molecular Dynamics Simulations. I. Cross-Linked Atomistic Models for Poly(methacrylate) Networks. *Comput. Theor. Polym. Sci.* **1998**, *8*, 169–178.

(18) Heine, D. R.; Grest, G. S.; Lorenz, C. D.; Tsige, M.; Stevens, M. J. Atomistic Simulations of End-Linked Poly(dimethylsiloxane) Networks: Structure and Relaxation. *Macromolecules* **2004**, *37*, 3857–3864.

(19) Wu, C.; Xu, W. Atomistic Molecular Modelling of Crosslinked Epoxy Resin. *Polymer* **2006**, *47*, 6004–6009.

(20) Varshney, V.; Patnaik, S. S.; Roy, A. K.; Farmer, B. L. A Molecular Dynamics Study of Epoxy-Based Networks: Cross-Linking Procedure and Prediction of Molecular and Material Properties. *Macromolecules* **2008**, *41*, 6837–6842.

(21) Odegard, G. M.; Jensen, B. D.; Gowtham, S.; Wu, J.; He, J.; Zhang, Z. Predicting Mechanical Response of Crosslinked Epoxy Using ReaxFF. *Chem. Phys. Lett.* **2014**, *591*, 175–178.

(22) Li, C.; Strachan, A. Molecular Simulations of Crosslinking Process of Thermosetting Polymers. *Polymer* **2010**, *51*, 6058–6070.

(23) Mortier, W. J.; Ghosh, S. K.; Shankar, S. Electronegativity-Equalization Method for the Calculation of Atomic Charges in Molecules. *J. Am. Chem. Soc.* **1986**, *108*, 4315–4320.

(24) Voter, A. F. Introduction to The Kinetic Monte Carlo Method. In *Radiation Effects in Solids*; Springer Netherlands: Dordrecht; pp 1–23.

(25) Platkowski, K.; Reichert, K.-H. Application of Monte Carlo Methods for Modelling of Polymerization Reactions. *Polymer* **1999**, *40*, 1057–1066.

(26) Romantsova, I. I.; Noa, O. V.; Taran, Y. A.; Yel'yashevich, A. M.; Gotlib, Y. Y.; Plate, N. A. Study of Intramolecular Crosslinking of Polymer Chains Using the Monte Carlo Method. *Polym. Sci. U.S.S.R.* **1977**, *19*, 3232–3241.

(27) Hamzehlou, S.; Reyes, Y.; Leiza, J. R. A New Insight into the Formation of Polymer Networks: A Kinetic Monte Carlo Simulation of the Cross-Linking Polymerization of S/DVB. *Macromolecules* **2013**, *46*, 9064–9073.

(28) Van Duin, A. C. T.; Dasgupta, S.; Lorant, F.; Goddard, W. A. ReaxFF: A Reactive Force Field for Hydrocarbons. *J. Phys. Chem. A* **2001**, *105*, 9396–9409.

(29) Stuart, S. J.; Tutein, A. B.; Harrison, J. A. A Reactive Potential for Hydrocarbons with Intermolecular Interactions. *J. Chem. Phys.* **2000**, *112*, 6472–6486.

- (30) Brenner, D. W.; Shenderova, O. A.; Harrison, J. A.; Stuart, S. J.; Ni, B.; Sinnott, S. B. A Second-Generation Reactive Empirical Bond Order (REBO) Potential Energy Expression for Hydrocarbons. *J. Phys.: Condens. Matter* **2002**, *14*, 783.
- (31) Ehlers, J.; Rondan, N. G.; Huynh, L. K.; Pham, H.; Marks, M.; Truong, T. N. Theoretical Study on Mechanisms of the Epoxy - Amine Curing Reaction. *Macromolecules* **2007**, *40*, 4370–4377.
- (32) Becke, A. D. Density-functional Thermochemistry. I. The Effect of the Exchange-only Gradient Correction. *J. Chem. Phys.* **1992**, *96*, 2155–2160.
- (33) Shenogina, N. B.; Tsige, M.; Patnaik, S. S.; Mukhopadhyay, S. M. Molecular Modeling Approach to Prediction of Thermo-Mechanical Behavior of Thermoset Polymer Networks. *Macromolecules* **2012**, *45*, 5307–5315.
- (34) Miron, R. A.; Fichthorn, K. A. Accelerated Molecular Dynamics with the Bond-Boost Method. *J. Chem. Phys.* **2003**, *119*, 6210–6216.
- (35) ASTM D792 - 13. *Standard Test Methods for Density and Specific Gravity (Relative Density) of Plastics by Displacement*. ASTM International: West Conshohocken, PA, 2013; p 6.
- (36) Chenoweth, K.; van Duin, A. C. T.; Goddard, W. a. ReaxFF Reactive Force Field for Molecular Dynamics Simulations of Hydrocarbon Oxidation. *J. Phys. Chem. A* **2008**, *112*, 1040–1053.
- (37) Ashraf, C.; van Duin, A. C. T. Extension of the ReaxFF Combustion Force Field toward Syngas Combustion and Initial Oxidation Kinetics. *J. Phys. Chem. A* **2017**, *121*, 1051–1068.
- (38) Russo, M. F.; Li, R.; Mench, M.; van Duin, A. C. T. Molecular Dynamic Simulation of Aluminum–water Reactions Using the ReaxFF Reactive Force Field. *Int. J. Hydrogen Energy* **2011**, *36*, 5828–5835.
- (39) Keten, S.; Chou, C.-C.; van Duin, A. C. T.; Buehler, M. J. Tunable Nanomechanics of Protein Disulfide Bonds in Redox Microenvironments. *J. Mech. Behav. Biomed. Mater.* **2012**, *5*, 32–40.
- (40) Chenoweth, K.; Cheung, S.; van Duin, A. C. T.; Goddard, W. A.; Kober, E. M. Simulations on the Thermal Decomposition of a Poly(dimethylsiloxane) Polymer Using the ReaxFF Reactive Force Field. *J. Am. Chem. Soc.* **2005**, *127*, 7192–7202.
- (41) Bedrov, D.; Smith, G. D.; van Duin, A. C. T. Reactions of Singly-Reduced Ethylene Carbonate in Lithium Battery Electrolytes: A Molecular Dynamics Simulation Study Using the ReaxFF. *J. Phys. Chem. A* **2012**, *116*, 2978–2985.
- (42) Fan, F.; Huang, S.; Yang, H.; Raju, M.; Datta, D.; Shenoy, V. B.; van Duin, A. C. T.; Zhang, S.; Zhu, T. Mechanical Properties of Amorphous Li X Si Alloys: A Reactive Force Field Study. *Modell. Simul. Mater. Sci. Eng.* **2013**, *21*, 074002.
- (43) Mortazavi, B.; Ostadhossein, A.; Rabczuk, T.; van Duin, A. C. T. Mechanical Response of All-MoS<sub>2</sub> Single-Layer Heterostructures: A ReaxFF Investigation. *Phys. Chem. Chem. Phys.* **2016**, *18*, 23695–23701.
- (44) van Duin, A. C. T.; Bryantsev, V. S.; Diallo, M. S.; Goddard, W. A.; Rahaman, O.; Doren, D. J.; Raymond, D.; Hermansson, K. Development and Validation of a ReaxFF Reactive Force Field for Cu Cation/Water Interactions and Copper Metal/Metal Oxide/Metal Hydroxide Condensed Phases. *J. Phys. Chem. A* **2010**, *114*, 9507–9514.
- (45) Zhang, W.; van Duin, A. C. T. Improvement of the ReaxFF Description for Functionalized Hydrocarbon/Water Weak Interactions in the Condensed Phase. *J. Phys. Chem. B* **2018**, *122*, 4083.
- (46) Plimpton, S. Fast Parallel Algorithms for Short-Range Molecular Dynamics. *J. Comput. Phys.* **1995**, *117*, 1–19.
- (47) Sirk, T. W.; Moore, S.; Brown, E. F. Characteristics of Thermal Conductivity in Classical Water Models. *J. Chem. Phys.* **2013**, *138*, 064505.
- (48) Littell, J. D.; Ruggeri, C. R.; Goldberg, R. K.; Roberts, G. D.; Arnold, W. A.; Binienda, W. K. Measurement of Epoxy Resin Tension, Compression, and Shear Stress–Strain Curves over a Wide Range of Strain Rates Using Small Test Specimens. *J. Aerosp. Eng.* **2008**, *21*, 162–173.